THE REAL MYSTERY - RELATING EEG MICROSTATES TO THE DEFAULT MODE NETWORK

Magnus Alexander Bitsch (s103243), Franciszek Olaf Zdyb (s093086), Anna Maria Walach (s121540)

Technical University of Denmark

ABSTRACT

An active area of research in neuroscience deals with characterizing the behavior of resting state networks (RSN), responsible for most of the energy consumption of the brain. In particular, the default mode network (DMN) has been hypothesized to correspond to mind-wandering, and linked to the pathology of mental disorders. The DMN is associated with slowly fluctuating hemodynamic signals (10 s). Analyses of EEG signals have revealed much shorter epochs (100 ms) of stable brain states, called microstates. Several studies have used simultaneous EEG and fMRI recordings to find a relation between the DMN and microstates, with conflicting results. Replicating the data-driven approach developed by Yuan et al., we applied microstate analysis to EEG recordings from 8 patients from Glostrup hospital, and attempted to predict the activation level of the DMN, as well as find the correlation between the microstates and other RSNs. We found no strong correlations.

Index Terms— machine learning, EEG, BOLD fMRI, microstates, Default Mode Network

1. INTRODUCTION

The aim of this project is to find a relation between EEG-derived microstates, and the Default Mode Network (DMN) from BOLD fMRI, using the method described in [Yuan et al., 2012].

Alterations in the DMN have been connected to various neurological diseases, like Alzheimers and schizophrenia [Yuan et al., 2012], [Khanna et al., 2015]. DMN is easily detected by fMRI scanning, but it is an expensive procedure requiring a visit to the hospital. If the DMN could be predicted using the EEG signal, it may allow the use of EEG as a cheaper and more portable tool for diagnosis of neurological diseases.

Microstates are unique topographic distributions of the electrical field potential in the brain [Khanna et al., 2015]. They are transient, patterned and quasi stable ($\sim$100ms). They are derived from the EEG signal using either temporal clustering or independent component analysis (ICA). Microstate analysis has been used for assessing the function of large-scale brain networks.

Default Mode Network Resting State Networks (RSNs) are networks of brain regions, that are active when a person is resting (but not sleeping). The Default Mode Network (DMN) is one of the most researched RSNs. Its subsystems include part of the medial temporal lobe for memory, part of the medial prefrontal cortex for theory of mind, and the posterior cingulate cortex for integration, along with the adjacent ventral precuneus and the medial, lateral and inferior parietal cortex [Buckner et al., 2008].

1.1. Research topic

The topic of this article consists of few subproblems:

- **artefact removal** - simultaneous recording of EEG and fMRI is causing a lot of noises in EEG signal. EEG is also very sensitive to heartbeat and eye and body movements. Removing artefacts is important part of feature engineering.

- **retrieving microstates** - different methods can be used to retrieve microstates from EEG [Khanna et al., 2015]. Establishing proper pipeline for retrieving microstates allows them to be robust and valuable features.

- **finding correlation** - once we obtain a features from EEG and values from fMRI, there are various tools that can be used to find correlation. Choosing a right one allows for finding hopefully high correlation with low bias.

1.2. Current status in literature

Although microstates analysis gathered more attention just recently, it was first described in [Lehmann and Skrandies, 1980]. This study showed that microstates are similar across subjects. It used method called *adaptive segmentation* to derive microstates, in which the topography at chosen time stamps is compared to the one before it, and considered the start of a new microstate if the centroid locations of the positive or negative potentials change by more than a predetermined amount [Khanna et al., 2015]. Right now studies are focusing on different method called *clustering analysis*, where the topographies from specific time stamps are used as an input for

clustering algorithm. It groups them in set of classes based on topographic similarity [Michel et al., 2009]. Recently, new method was proposed that uses independent component analysis to find microstate classes [Yuan et al., 2012].

Number of studies that tries to correlate EEG with fMRI is growing and microstate analysis is a popular tool to use in such projects. We can observe some promising results [Yuan et al., 2012], that allows to assume the correlation is significant and can be found.

2. DATA

The EEG and fMRI data were recorded simultaneously.

The data contains 10 minutes probes from 20 subjects, recorded in free different settings: in atmospheric, increased CO_2 and increased O_2 conditions. It was recorded in Glostrup Hospital by Egill Rostrup and Ulrich Lindberg as a simultaneous EEG/fMRI. The recording included 30 electrodes for brain activity measurement, one for eye movement and one for heartbeat. The sampling frequency was 500 Hz. The time stamp of launching the fMRI is recorded for each sample, so the data can be trimmed appropriately.
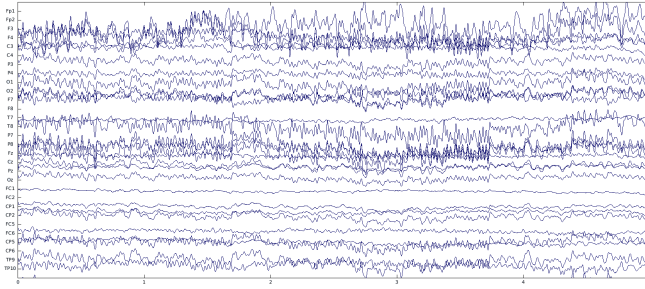

Fig. 1. Time courses from EEG.

2.1. Artefact removal

Initial cleaning of the data, especially removing the fMRI artefacts, has been performed by Glostrup Hospital staff, followed by further artefact removal performed by Andreas Trier Poulsen. This process included notch- and low-pass filtering, as well as using ECG and EOG to get rid of eye blinks and heart beat artefacts. The data from only 5 subjects (in all conditions) remained.

3. GENERATING MICROSTATES

The input data for this process is artefact-free data from five subjects in all conditions, from 30 electrodes. At the end, we have 30 microstates, from which some will be chosen as regressors in correlation task.

3.1. Global Field Power

Following Yuan et al., we calculated the Global Field Power time course (GFP), which is a standard deviation across electrodes. Then we found topographies corresponding to peaks in the GFP. The parameters of the peak detection algorithm were selected for highest correlation with the fMRI data via a grid search.
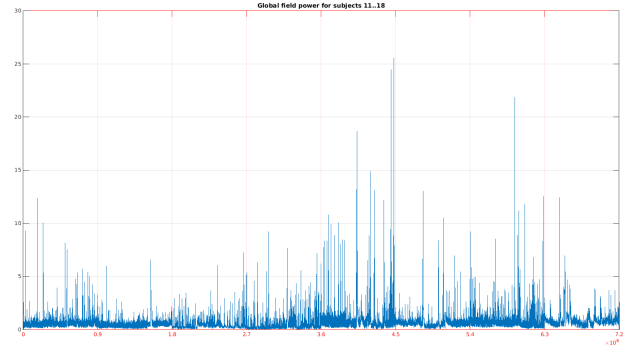

Fig. 2. Global Field Power.

3.2. Independent Component Analysis

We concatenated the topographies from peaks across subjects, and run ICA. Our algorithm of choice was FastICA [Hyvarinen, 1999] with the cubic non-linearity function. The resulting separation matrix was applied to the continuous EEG to obtain time courses of the microstates.
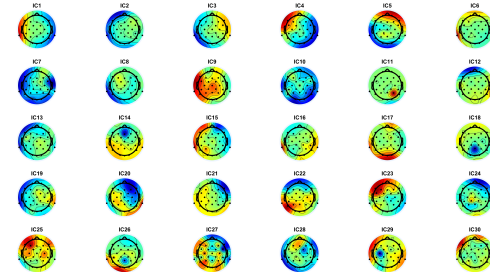

Fig. 3. Spacial images of microstates derrived from ICA.

3.3. Hemodynamic response function

We constructed a binary matrix which encodes which microstate has the highest activation at each time, and convolved it with the hemodynamic response function to adjust for the time-delay of the BOLD fMRI response. These were used as regressors in the elastic net model [Hastie et al., 2009].

4. CORRELATION OF MICROSTATES AND DMN

In this section, we describe proccess of finding the best subset of microstates time course used for predicting the DMN activity and the predicting algorithms.

We assumed that each subject is independent and further that microstates are common states across subjects as suggested in [Yuan et al., 2012]. This allowed us to concatenated data from different subjects and perform model selection based on a larger data set.

There are two kinds of input for algorithms in this section:

- **Microstate time series**, described in previous section

- **DMN Independent Components (DMN ICs)** from BOLD fMRI. We received time series of 60 fMRI components from Glostrup Hospital. Two of them represents activity of DMN. The sample rate is $\frac{1}{3} Hz$.
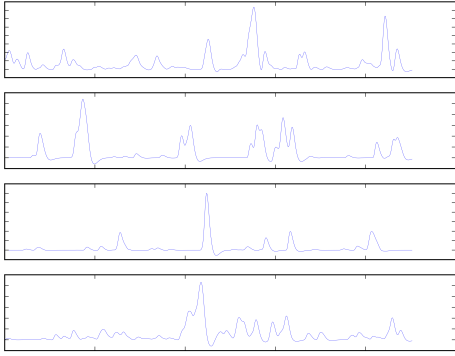

Fig. 4. Microstates time course used as regressors. Shown are four out of thirty time courses.

4.1. Elastic net

As suggested in the literature [Yuan et al., 2012], each RSN is related with one or a combination of several microstates. Yuan identified 13 microstates related to 10 different RSN. We wished to find which of the microstates time course that characterizes the default mode network. Performing both feature selection and variance reduction, by shrinking the coefficients in imposing a penalty on the coefficients, the elastic-net (EN) model [Hastie et al., 2009] provides a framework for describing the relation between the EEG microstates and the DMN IC. The elastic-net selects variables like the lasso, and shrinks together the coefficients of correlated predictors like ridge [Hastie et al., 2009]. The elastic net penalty is given in (1).

$$\lambda \sum_{j=1}^{p} \left(\alpha |\beta_j| + (1 - \alpha)\beta_j^2 \right) \tag{1}$$

The elastic-net is implemented with the least angle regression (LAR) method. The full path of the LAR with $\lambda = 0$ yields the general linear model.

4.2. Cross-validation

Estimating the EN-penalty in (1) we performed 5-fold cross-validation using all the artefact corrected data of the 8 subjects. However, since this is a limited amount of data we did not set a side a independent test. We chose to randomly divide the data into the 5 folds to adjust to the fact that the behaviour of a subject might 'change' over time in the scanner e.g. fall asleep. Hence, we limit the correlation in time between the training data and test data. However, since we did not have an independent test set, we could not assess the generalization error. Instead, we estimated the error on the validation set.

4.3. Model and peak size

The GFP is an sensitive measure and it is not clear whether all local peaks of the GFP should be included as input in estimating the decomposition matrix, which is later applied on the entire time course of the EEG signal. The local peaks of the GFP can be seen as 'raw' microstates. We performed a grid search altering the minimum width and height of the peaks. The width and height was linearly spaced between 0 and 100 ms, and max(GFP)/2 respectively, constraining the transient brain state (peak) to be quasi stable near 100 ms. It would have been ideal to use the validation error of the EN to find the optimal design settings in the peak detection. However, it has shown to be a very hard task to predict the DMN, Instead, we used the design setting in which gave the single maximum correlation of one time course of a microstate with the DMN in the EN model. We performed 5-fold cross-validation with λ log-spaced in the interval $[\,10^{-4}\,;\,10^{2}\,]$ in estimating the EN model.

4.4. Robustness of the microstates

In order to evaluate the robustness of the algorithm of finding microstates, we altered the minimum peak width and height, as described above, in the peak detection and performed 5-fold cross validation omitting one subject at each fold. In each fold, for a specific set of parameters in the peak detection, we found a set of microstates ordered by the power explained. We aligned the matrices to be of the same sign using correlation of the first column of the mixing matrices with respect to the first fold. We compared the sum of the Frobenius norm of the deviation from the mean of the mixing matrices. We found that the robustness decreased in both directions. Hence, no restrictions should be given for the peak detection algorithm for the maximum robustness.

5. RESULTS

Correlation. In the grid search of the optimal parameters for the peak detection we found that using a minimum sampling length of 100 ms gave the highest correlation. The two com-
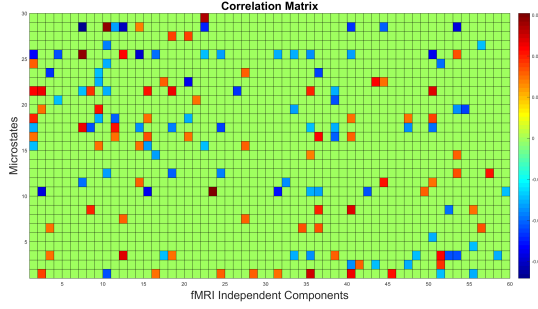
Fig. 5. Correlation matrix between microstates (Y axis) and ICs of fMRI (X axis). The correlation is thresholded at the significance level of $p < 0.05$ (uncorrected).

ponents DMN ICs, IC3 and IC7, had 3 and 5 significant correlations respectively on the level of $p < 0.05$. On the level of $p < 0.001$ this was reduced to 1 and 2 significant correlations respectively (see 7 in the appendix). We found a maximum correlation of -0.0682

Model. The elastic net found that 10-18 microstates is the optimal number of regressors. The best run we have found was using 13 microstates as regressors which is shown in figure 6 with IC7 of the fMRI data as the response variable. Here we found the optimal tuning parameter ($\lambda = 2.6561$) which means that we have a penalty on the size of parameters in the elastic net model. The normalized mean square error is 0.9928, where a value of 1.0 corresponds to predicting the mean." The selected topographies are shown in the appendix in figure 9.
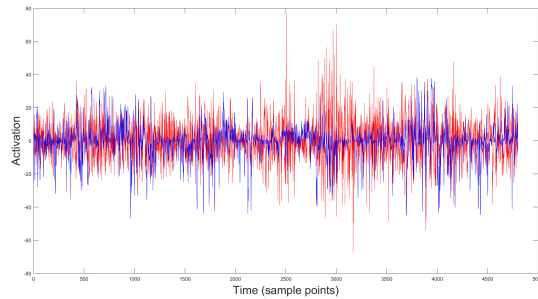

Fig. 6. Predicting DMN signal. DMN IC (IC7) (red line) and prediction by microstates (blue line).

6. DISCUSSION

In this work we investigated the relation between the EGG microstates to the DMN IC, which has shown to be a very challenging quest. After artefact correction and altering various parameters and algorithms the MSE over the variance is still close to one. However, it has been shown that there

is correlation between the EEG microstates and the DMN IC but the relation has not yet been fully uncovered.

In general it was found that between 10 and 18 microstates was selected by the EN using the validation error. The quality of the prediction is rather low which makes this variable selection sensitive.

Comparing results with Yuan. [Yuan et al., 2012] identified 13 microstates related to 10 different RSN. Yuan found 3 EEG microstates significantly ($p < 0.001$ (uncorrected)) correlated with the DMN IC. We found 1 and 2, respectively for the two DMN IC. The magnitude of the correlations found in our experiment corresponds well to the ones found by Yuan. Comparing the maximum correlation of the DMN IC in [Yuan et al., 2012] and in our experiment it seems that Yuan had a slightly higher maximum correlation of about twice the size of ours.

Comparing the microstates topography Comparing fig. 3 in [Yuan et al., 2012] it is seen that

Selecting the design parameters. The peak detection design settings of the GFP, we choose the setting with the one microstate that was maximally correlated with the DMN IC. This gives the maximal correlated single time course design setting, however, makes the measure sensitive. One could instead use two or more time courses for the correlation for the optimal design setting, however as suggested in the literature [Yuan et al., 2012], each RSN is related with one or a combination of several microstates. It is therefore not clear whether a more robust measure is to be preferred, since a satisfactory measure of the test error has not been found.

7. CONCLUSIONS

We have shown that the temporally slow hemodynamic fluctuations of the BOLD default mode network is correlated with the temporally fast, spontaneous electrophysiological activity reflected in the EEG microstates followed by the approach in [Yuan et al., 2012]. However, the magnitude of the found correlation, even though significant, is not too satisfactory. A model for predicting the signal has been postulated with 13 microstate time courses as regressors. The varying number of included microstates and high prediction error leaves room for further work in investigating the relation between the EEG microstates and the default mode network, to fully uncover the relation.

8. ACKNOWLEDGEMENTS

9. REFERENCES

[Buckner et al., 2008] Buckner, R. L., Andrews-Hanna, J. R., and Schacter, D. L. (2008). The brain's default network: Anatomy, function, and relevance to disease. *Annals of the New York Academy of Sciences 1124 (1): 138*.

[Hastie et al., 2009] Hastie, T., Tibshirani, R., and Friedman, J. (2009). *The Elements of Statistical Learning. Data Mining, Inference, and Prediction, Second Edition*. Springer-Verlag New York.

[Hyvarinen, 1999] Hyvarinen, A. (1999). Fast and robust fixed-point algorithms for independent component analysis. *Neural Networks, IEEE Transactions on*, 10(3):626–634.

[Khanna et al., 2015] Khanna, A., Pascual-Leone, A., Michel, C. M., and Farzan, F. (2015). Microstates in resting-state eeg: Current status and future directions. *Neuroscience & Biobehavioral Reviews*, 49(0):105 – 113.

[Lehmann and Skrandies, 1980] Lehmann, D. and Skrandies, W. (1980). Reference-free identification of components of checkerboard-evoked multichannel potential fields. *Electroencephalography and clinical neurophysiology*, 48(6):609–621.

[Michel et al., 2009] Michel, C. M., Koenig, T., and Brandeis, D. (2009). Electrical neuroimaging in the time domain. In Michel, C. M., Koenig, T., Brandeis, D., Gianotti, L. R. R., and Wackermann, J., editors, *Electrical Neuroimaging*, pages 111–144. Cambridge University Press. Cambridge Books Online.

[Yuan et al., 2012] Yuan, H., Zotev, V., Phillips, R., Drevets, W. C., and Bodurka, J. (2012). Spatiotemporal dynamics of the brain at rest exploring eeg microstates as electrophysiological signatures of bold resting state networks. *NeuroImage*, 60(4):2062 – 2072.
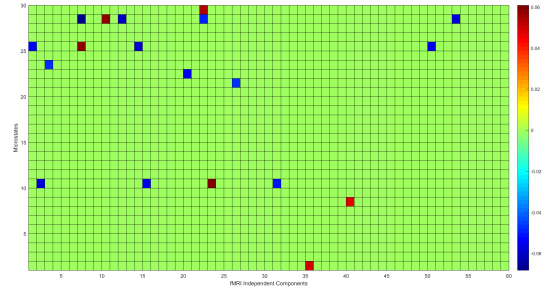
FOR THE APPENDIX

Fig. 7. Correlation matrix between microstates (Y axis) and ICs of fMRI (X axis). The correlation is thresholded at the significance level of $p < 0.001$ (uncorrected).
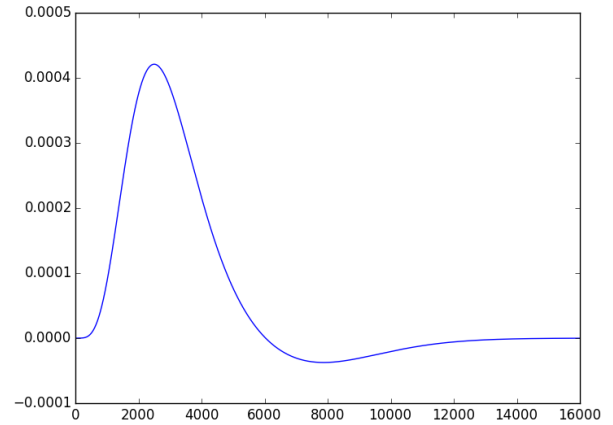

Fig. 8. Hemodynamic response function used in the project.

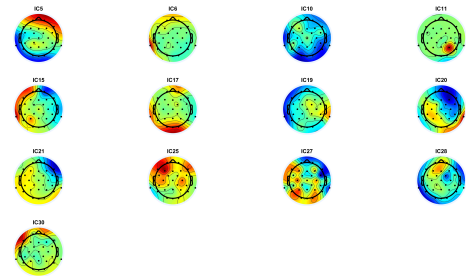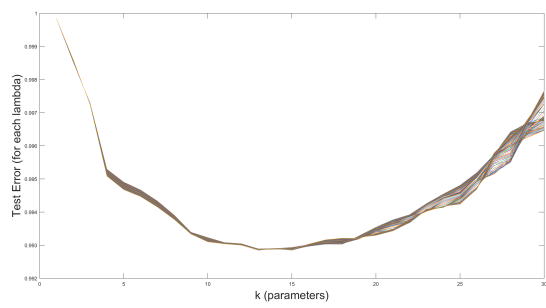**Fig. 9**. The 13 slected regressors by the elastic-net shown as topographies.

Fig. 10. Selection of parameters. Each line corresponds to a λ. It is seen that 13 regressors produces the lowest error.